EUROPHYSICS LETTERS

Helicase activity on DNA as a propagating front

* * *

S. M. Bhattacharjee

Published under the scientific responsibility of the

EUROPEAN PHYSICAL SOCIETY

EUROPHYSICS LETTERS

Taking full advantage of the service on Internet, please choose the fastest connection:

http://www.edpsciences.org
http://edpsciences.nao.ac.jp
http://edpsciences-usa.org
http://www.epletters.ch

Europhysics Letter was launched more than fifteen years ago by the European Physical Society, the Société Française de Physique, the Società Italiana di Fisica and the Institute of Physics (UK) and owned now by 17 National Physical Societies/Institutes.

Europhysics Letters aims to publish short papers containing non-trivial new results, ideas, concepts, experimental methods, theoretical treatments, etc. which are of broad interest and importance to one or several sections of the physics community.

Europhysics letters provides a platform for scientists from all over the world to offer their results to an international readership.

Institution/Library: . . . .
. . . .
Name: . . . .
Position: . . . .
Address: . . . .
. . . .
. . . .
ZIP-Code: . . . .
City: . . . .
Country: . . . .
E-mail: . . . .

Signature :

Helicase activity on DNA as a propagating front

S. M. BHATTACHARJEE[1](*)

[1] *Institute of Physics - Bhubaneswar 751 005, India*

Abstract. – We develop a propagating-front analysis, in terms of a local probability of zipping, for the helicase activity of opening up a double-stranded DNA (dsDNA). In a fixed-distance ensemble (conjugate to the fixed-force ensemble), the front separates the zipped and unzipped phases of a dsDNA and a drive acts locally around the front. Bounds from variational analysis and numerical estimates for the speed of a helicase are obtained. Different types of helicase behaviours can be distinguished by the nature of the drive.

A helicase moves along a DNA and unwinds it. Whenever a double-stranded DNA in a cell needs to be opened up, a helicase is summoned, be it during the semi-conservative replication, repair mechanism of a stalled process or other DNA-related activities [1]. A large number of helicases, including rna-helicases, have so far been identified from different pro- and eucaryotes. A well-studied bacterium like *E. coli* contains at least 17 different helicases, though the need and the function of each of these are not yet clear.

The helicase activity involves a motor action fed by NTPs (nucleotide triphosphate) and eventual opening of DNA by dissociating successive base pairs along the chain [2]. Quantitative estimates of rates of such activities (~ 400 base pair per second or less) for almost all helicases are known from *in vitro* studies in solutions and more recently from single molecular experiments. Attempts to categorize these varieties of helicases as per their common features have led to various classification schemes. These are: i) active *vs.* passive depending on the direct requirement of NTP for the opening; ii) families and superfamilies (SF) based on the conserved motifs of the primary sequence; iii) monomeric, dimeric, hexameric, oligomeric depending on the number of units required for activity; and iv) mode of translocation: whether it translocates on the single strands of DNA or on dsDNA. For example, dnaB, the main helicase involved in the replication of DNA in *E. coli*, is a hexameric, passive helicase belonging to the dnaB-like family translocating on a single-strand DNA [3]. PcrA is an active, SF1, monomeric helicase translocating on ssDNA [4], while recG is an active, SF2, monomeric, dsDNA translocating helicase [5]. Apart from these gross classifications, very little information is available on the detailed mechanism of the helicase activity.

Crystallographic data available for a few helicases have been used to model mechanisms for specific helicases. Though crystal structures cannot give a dynamic view, such proposals, attractive no doubt, are the only ones available so far. According to these proposals, a hexameric helicase like dnaB opens up dsDNA like a wedge by virtue of its motor action on
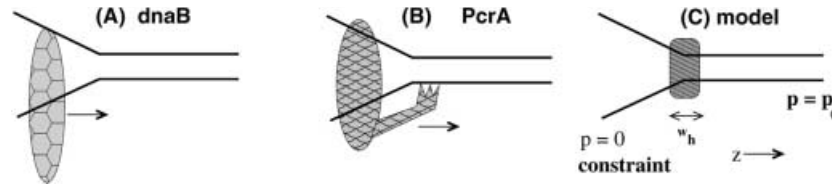
(*) E-mail: `somen@iopb.res.in`

Fig. 1 – Schematic representation of the advocated mechanisms for (A) dnaB and (B) PcrA helicases (see text) whose motions are indicated by the arrows. (C) Proposed model. Constraints are that the DNA is open on one side but zipped on the other, both phases coexisting. The unzipped phase is preferred within the shaded box of width w_h encompassing the Y-fork or interface or domain wall.

ssDNA [3]. A rolling mechanism has been proposed for dimeric helicases [6]. In case of PcrA, the helicase activity and the motor action can be decoupled. Crystal structure, supplemented by biochemical evidences on mutants, favours a mechanism where the helicase moves forward on ss-DNA and during its sojourn a different domain of the helicase pulls a few bases of a strand of the ds-DNA beyond the Y-fork, the junction between ss and ds-DNA [4]. See fig. 1 for a schematic diagram. RecG is more complicated because it moves in opposite direction from zipped to unzipped, a fork reversal process forming a Holliday junction of 4 DNA strands [5].

   Our aim is to develop a generic physical picture that could be applicable to all the different types of helicases. Recently, a phase-coexistence–based mechanism for helicase activity has been proposed by Bhattacharjee and Seno [7]. A kinetic model has also been proposed recently [8] while a random walk model was used in an earlier study [9] to analyze the movement on DNA. The phase-coexistence mechanism is based on the unzipping phase transition of a ds-DNA by a force, which was first shown in a continuum model in ref. [10]. This transition has since then been established by exact calculations for lattice models in all dimensions [11, 12], in studies of dynamics [11, 13], by scaling theories [14], in quenched averaged DNA [15], and others. The key points of the mechanism [7] are the following. a) A helicase keeps two single strands of a dsDNA at a separation much bigger than the base-pair separation of a ds-DNA. b) The resulting fixed-distance ensemble for a dsDNA breaks it up into a zipped phase and an unzipped phase separated by a domain wall. c) The domain wall is identified as the Y-fork junction. All helicases act at or near this junction of the ds-ss DNA. d) The motor action of the helicase leads to a shift in the position of the fixed-distance constraint thereby shifting the domain wall towards the zipped phase. Additional features are needed for efficiency, job-requirement and processivity (the distribution of the length unzipped before a helicase drops off). Our purpose in this paper is to use this coexistence hypothesis to develop a simple coarse-grained model of the propagation of the Y-fork.

   We use the zipping probability $p(z)$, the probability that the base pair at index or contour length z (measured along the backbone) is zipped, as the basic variable. The unzipping transition by a force has hitherto been studied by using polymer models. However, in the case of the conjugate fixed-distance ensemble, the probability of zipping, $p(z)$, under the imposed constraints, has been shown to be a useful description [7, 16]. In the polymer approach, one introduces a local variable $n(z) = 1$ or 0 depending on whether the base pairs at z are bound or not to write the pairing energy, characteristic of the DNA problem, as $\int dz \epsilon(z) n(z)$, where $\epsilon(z)$ is the base pairing energy at z. The average value $\langle n(z) \rangle$ gives the fraction p_0 of bound base pairs, and it is the parameter monitored in melting and unzipping transitions. This suggests the use of $p(z)$ as a coarse-grained parameter to use for the inhomogeneous case, especially for the description of the interface. Since the unzipping transition is of first-order nature with a co-existence on the phase boundary, and our interest is in the region much
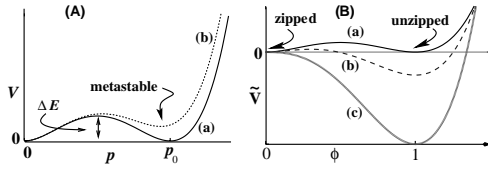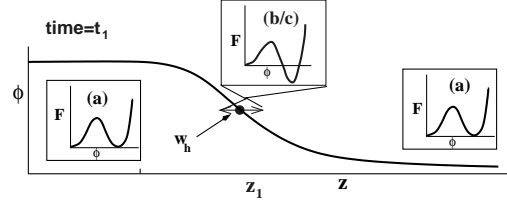
Fig. 2

Fig. 3

Fig. 2 – Plots of (A) $V(p)$ and (B) $\tilde{V}(\phi)$. Curves (a) show the co-existence of the zipped ($p = p_0$ or $\phi = 0$) and the unzipped ($p = 0$ or $\phi = 1$) phases. Curves (b) and (c) show the change near the interface or domain wall due to the drive (h in eq. (4)) that makes the zipped phase locally metastable or unstable.

Fig. 3 – Schematic representation of the pulse. The front is at location z_1 (filled circle at $\phi = 0.5$) at an arbitrary time t_1. The effective free energy is of form (b) or (c) of fig. 2 (metastable or unstable) only within $z_1 \pm w_h$. The drive or pulse moves with the front. The relaxation due to the elastic term leads to a traveling-wave solution.

below the thermal melting point of DNA, a phenomenological Landau-type Hamiltonian or free energy can be used to describe the state of the DNA. In addition, the presence of the helicase can be represented by the boundary conditions on two sides of the DNA (zipped on one side and unzipped on the other). The effect of the motor action that pushes (or pulls) one phase into the other and any other destabilizing effects of the helicase are taken into account by additional terms involving the zipping probability $p(z)$. We show the existence of a traveling-wave solution (*i.e.* a propagating front of Y-fork) and then get the speed of the front in terms of the parameters of the Hamiltonian. A variational principle is used to derive bounds on the selected velocity.

The unzipping transition can be described by a Landau-type Hamiltonian or free energy,

$$H_0 = \int \mathrm{d}z \left[\frac{K}{2} \dot{p}(z)^2 + V(p(z)) \right], \quad \text{with} \quad V(p) = \frac{1}{2} r p^2 + \frac{1}{3} w p^3 + \frac{1}{4} u p^4, \tag{1}$$

where K is the appropriate rigidity modulus, $\dot{p}(z) = \partial p(z)/\partial z$, and the cubic term ensures a first-order transition for $w < 0$, $u > 0$. See fig. 2. The coefficients r, w and u can in principle be determined from the knowledge of the unzipping phase boundary and p_0. It is often useful (and used here also) to reparametrize $V(p)$ in terms of p_0, the width of the well at p_0 and the barrier height ΔE. By treating eq. (1) as the mean-field free energy [17], the dynamics of unzipping is given by the overdamped equation of motion

$$\Gamma^{-1} \frac{\partial p(z)}{\partial t} = -\frac{\delta H_0}{\delta p(z)} \tag{2}$$

with appropriate transport coefficient Γ. Since we are away from critical points and interested in the nonequilibrium propagation problem, we may ignore noise terms in the equation of motion. Stochastic terms would also be required to describe processivity, which we do not consider in this paper.

For a long chain, with the boundary conditions $p(z) \to p_0$ (probability in the zipped phase) as $z \to +\infty$ and $p(z) \to 0$ as $z \to -\infty$ at phase coexistence, the variation of the equilibrium probability of zipping is described by the equation $K\ddot{p}(z) = V'(p)$, with prime (dot) denoting derivative with respect to the argument (z). For the assigned boundary condition, there is a domain wall solution located at an arbitrarily chosen $z = 0$ with a profile

$\int_0^p \mathrm{d}p/\sqrt{2V(p)/K} = z$, and $p(z)$ approaches the bulk value exponentially in the zipped phase as $p_0 - p(z) \sim \exp[-V''(p_0)|z|/\sqrt{K}]$. The energy of a wall of width W, in terms of the barrier height ΔE (fig. 2), is $E = K\frac{p_0^2}{W} + \Delta E W$, which, on minimization, gives $W = (Kp_0^2/\Delta E)^{1/2}$. Measurements of W, and of ΔE (from the decay rate of bubbles in the bound state) would give an estimate of K. This equilibrium situation can be obtained by keeping the helicase static on dsDNA, *e.g.* by denying ATP in *in vitro* experiments. Since such configurations can now be prepared [18], detailed characterization of the wall can be done experimentally.

In order to incorporate the effect of the motion of the helicase, we introduce a moving perturbation that tends to destabilize the domain wall at its current location. A time-dependent perturbation is introduced in the equation of motion, eq. (2) or, equivalently, in the Hamiltonian of eq. (1), that favours the unzipped state over a region of width w_h around the domain wall, maintaining co-existence elsewhere. See figs. 2 and 3. The crystal structure of PcrA [4] suggests that $w_h \sim 20$ bases. The equation of motion, augmented by a "drive" term, is now given by

$$\Gamma\frac{\partial p(z)}{\partial t} = K\frac{\partial^2 p}{\partial z^2} - rp + wp^2 - up^3 - h(z,t)V_1'(p), \quad \text{with} \quad h(z,t) = \mathcal{U}\left(\frac{z-ct}{w_h}\right). \quad (3)$$

This is equivalent to adding a term $\int \mathrm{d}z\,h(z,t)V_1(p)$ in the Hamiltonian, eq. (1), such that the drive favours the unzipped region ($p = 0$) in a region of width w_h around $z = ct$, with the front position at $t = 0$ chosen as origin $z = 0$. In eq. (3), $V_1(p)$ should have the right form for $V(p) + V_1(p)$ to favour the unzipped phase. Since the helicase works only near the interface or the front, $\mathcal{U}(x)$ is a short-range function. For simplicity, we choose $\mathcal{U}(x) = \Delta u$ for $|x| \leq 1$ and zero otherwise. The "drive" is attached to the front and moves to the zipped side with a speed c which is to be determined self-consistently so that the front also moves with the same speed.

The role of the drive term is to disturb the coexistence between $p = 0$ (unzipped) and $p = p_0$ (zipped phase). By a transformation of variables, like $p = p_0 - \phi$ and rescaling, we recast eq. (3) in a more standard and symmetrical form (by choosing $V_1(p)$):

$$\frac{\partial \phi(z)}{\partial t} = \frac{\partial^2 \phi}{\partial z^2} + f(\phi), \quad \text{where} \quad f(\phi) = \left(-\frac{1}{3} + h(z,t)\right)\phi + \phi^2 - \left(\frac{2}{3} + h(z,t)\right)\phi^3, \quad (4)$$

and, for brevity, same notation h is used for the drive. Another choice could have been $f(\phi) = \phi(1-\phi)(\phi - \frac{1}{2} - h(z,t))$ which is identical to eq. (4) up to a scale transformation if and only if $h = \text{constant}$. In any case no fundamental difference is expected among the various possible choices. Equation (4) allows the zipped phase with $\phi = 0$ and the unzipped phase with $\phi = 1$ for all h. These two phases coexist at $h = 0$, while $\phi = 0$ is metastable for $0 < h < 1/3$ and unstable for $h > 1/3$. See fig. 2. The symmetrical form helps in identifying the location of the front by $\phi = 0.5$ and the drive $h(z,t)$ is operative only around that point.

Assuming that the front propagates with a velocity c, *i.e.* $\phi(z,t) = \phi(z-ct)$, we can use the comoving frame with coordinate $\xi = z - ct$ to rewrite eq. (4) as

$$\frac{\partial^2 \phi}{\partial \xi^2} + c\frac{\partial \phi(z)}{\partial \xi} + \frac{\partial}{\partial \phi}\tilde{V}(\phi) = 0, \quad \text{with} \quad \frac{\partial}{\partial \phi}\tilde{V}(\phi) = -f(\phi), \quad (5)$$

which has a mechanical analogy of a particle moving in a potential $-\tilde{V}(\phi)$ under friction (taking ξ as a timelike variable). This analogy immediately tells us (using first integral or energy conservation) that to satisfy the boundary conditions at $\xi = \pm\infty$ when $h = 0$, one must have $c = 0$. In other words, there is no propagating solution as it should be in the case of phase coexistence. A propagating solution ensues if the drive h is not zero, with $c = c(\Delta u, w_h)$.

The speed of propagation c has to be insensitive to the width w_h of the pulse if $w_h \gg$ the width of the front or interface. In that large w_h limit, c should be the speed of a propagating front for a uniformly metastable (*i.e.* $h < 1/3$) or unstable (*i.e.* $h \geq 1/3$) case. We recollect the relevant results for the uniform situation with $h(z,t) =$ constant. i) There is a pushed-to-pulled transition [17] in the propagation of the front at $h = 4/3$. ii) Beyond $h = 4/3$, the velocity is determined by the linearized equation of motion while the full nonlinearity is important for $h < 4/3$. iii) For the metastable case ($h < 1/3$), any initial condition $\phi_0(z) = \phi(z, t = 0)$ rapidly evolves to a steady shape with a velocity $c^\dagger(h) = 3h/\sqrt{2[(2/3) + h]}$, approaching the steady speed exponentially fast in time. iv) For the unstable case, a sharp interface (say a sharp step at $t = 0$) also evolves to this "pushed" front so long as $h \leq 4/3$. However, a flatter interface would maintain its flatness and move with a speed determined by the initial flatness. v) In the pulled limit ($h > 4/3$), the asymptotic speed is the linearized speed $c^*(h) = 2\sqrt{h - (1/3)}$ which is reached algebraically in time, provided the initial condition is sharp (*e.g.*, a step function).

With a pulse, one may use the particle mechanics analogy that a particle is in one of the peaks of the equal-height double-peaked potential $-\tilde{V}(\phi)$ at $\xi = -\infty$ and then at finite time it gets a push (energy input in particle mechanics) which should be sufficient to overcome frictional loss and reach the other peak at $\xi = +\infty$. This will satisfy the boundary conditions at $\xi = \pm\infty$. A moving front is therefore possible. In other words, the moving front originates from the "elastic term" that tries to spread out the change in ϕ in the front region.

For a quantitative analysis of the speed, we use a variational principle [19]. If the equation of motion admits, as we verify numerically below, a monotonic front $\phi(z,t) = q(\xi)$, then the inverse mapping can be used to get ξ from q with $0 \leq q \leq 1$. There is an inequality,

$$c^2 \geq 2 \frac{\int_0^1 fg \, \mathrm{d}q}{\int_0^1 -(g^2/g') \mathrm{d}q} \,, \tag{6}$$

for any positive function $g(q)$ with $-\mathrm{d}g/\mathrm{d}q > 0$, provided the integrals exist. This requires $f'(0) < 0$ for bistable f of the form eq. (4). Only the metastable case is considered here. The unstable case with $f'(0) > 0$ can also be treated though in a slightly different way. Taking $g(q) = [(1-q)/q]^b$ and the uniform case of f, *i.e.* $h(z,t) = h$, one gets

$$c^2 \geq \big(-b^2/3\big) + hb(6-b)/2. \tag{7}$$

The supremum of the lower bound at $b = 9h/(2+3h)$ recovers the exact velocity, $c^\dagger$, mentioned earlier (valid for $h < 1/3$). Under the assumption of monotonicity, the pulse, in q-space, is at $q = 1/2$ and is of width $\Omega(w_h)$ such that $\Omega(w_h \to \infty) = 1/2$. The profile $q(\xi)$ generally approaches the two limits exponentially, as we have seen earlier, and therefore $\tilde{\Omega} \equiv (1/2) - \Omega \sim \exp[-w_h/w^*]$ with some characteristic length w^*. The pulse term contribution to the numerator of the bound of eq. (6) is an integral of $q(1-q^2)g(q)$ over $q \in [\tilde{\Omega}, 1 - \tilde{\Omega}]$ and the integral can be expressed in terms of incomplete beta-functions. We then obtain

$$c^2 \geq \frac{-b^2}{3} + \frac{1}{2}\Delta ub(6-b) - A\big(\tilde{\Omega}, b\big)\Delta ub, \tag{8}$$

where the form of $A(\tilde{\Omega}, b)$ (≥ 0) is not displayed. Taking the maximum of the right-hand side as the best estimate $c(\Delta u, w_h)$ for the speed, we see that $c(\Delta u, w_h) < c^\dagger$ (the bulk value), as expected. Using the asymptotic behaviour of the incomplete beta-functions in $A(\tilde{\Omega}, b)$, one finds that $c(\Delta u, w)$ saturates exponentially for large w_h. In the other limit of small w_h (equivalent to small Ω), there is a linear dependence on w_h. Combining these, we may write $c(\Delta u, w) = c_0[1 - a \exp[-w/w_0]]$, a form that does represent the numerical data very well.
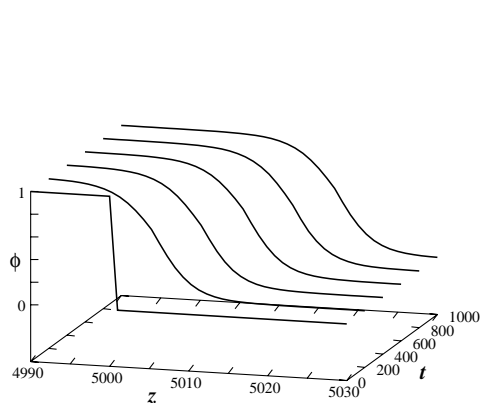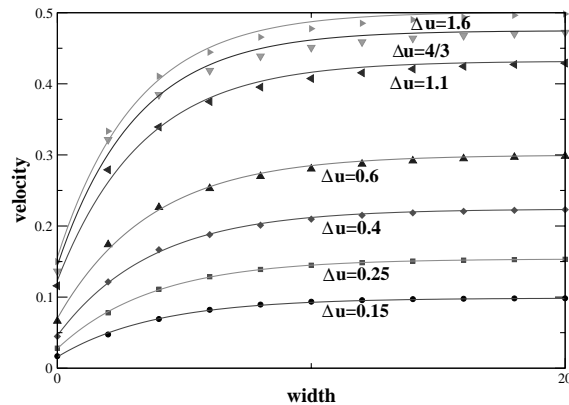
Fig. 4

Fig. 5

Fig. 4 – Positions of the front or domain wall for $\Delta u = 0.2$ (see below eq. (3)) at bulk coexistence are shown by plotting $\phi(z)$ *vs.* z. The curves are at times 0, 200, 400, 600, 800, 1000 in arbitrary time units and are obtained from a discretized version of eq. (4).

Fig. 5 – Plot of $c(\Delta u, w_h)$ as a function of the width w_h of eq. (3) for different values of Δu as noted against the curves. Solid lines are fits to $c(\Delta u, w) = c_0[1 - a \exp[-w/w_0]]$.

In order to determine the velocity of propagation of the front with a pulse, we have numerically solved a discretized version of eq. (5) for various values of the width w_h and magnitude of the drive Δu. A small time step is chosen for proper convergence but no spatial continuum limit has been done. We start with a sharp interface, $\phi = 1$ for $0 \leq z \leq L/2$ and $\phi = 0$ for $z > L/2$. A sequential update is done. At every time step, we allow a square pulse of width w_h and strength Δu at the current location of the domain wall or front (located by $\phi = 0.5$). In all cases we observed a monotonic front. Figure 4 shows the time evolution of the front for the case of a drive with $\Delta u = 0.2$ and of zero width, $w_h = 0$ (pulse at one point of the lattice only).

The variation of the speed with the width of the pulse is shown in fig. 5. Consistent with our results from the variational analysis, we see that the velocity approaches the bulk limit for large widths and this approach is exponential. There is a small but systematic deviation of the observed velocity from the exponential fit for larger values of Δu (in the "unstable" region). Detailed analysis of the pushed *vs.* pulled cases will be reported elsewhere.

In terms of helicases, it seems natural to associate dnaB-type passive helicases with the metastable case where the motor action provides the drive that locally disturbs the Y-fork region. As in ref. [7], we identify the domain wall or the front as the Y-fork region —the junction of the ds-ss DNA. In the metastable case, the pushed dynamics has a stability against small fluctuations, the speed of propagation is independent of the initial conditions, and the speed approaches the steady-state limit exponentially in time. All of these are important properties expected of a helicase of dnaB-type which, after loading on DNA, carries out the unzipping in tandem with the other processes during replication.

So far as PcrA (fig. 1) is concerned, we associate the overall dynamics to the unstable case. No quantitative experimental results are available regarding the magnitude and width of the force PcrA exerts on the bases beyond the Y-fork. It is reasonable to assume that the force is meant to unzip DNA locally, and the effect of this pulling is to make the ds-region unstable. We then infer that PcrA operates in the unstable ($h > 1/3$) regime. In several

mutants of PcrA (replacing a few residues by alanines) the helicase activity (the hand in fig. 1) could be decoupled (reduced) from the motor action and ATP intake (both remained more or less the same). In our terminology, these mutations involve a reduction in h (*i.e.* the overall pulling strength, Δu, or the width of the pulse, w_h, or both), producing a reduction in the speed as shown in fig. 5. We would like to add that reversed motion of recG can also be understood in the same scheme with a few extra ingredients. This will be discussed elsewhere. Active helicases like PcrA that are involved in repair processes become operational when the replication process stalls because of, *e.g.*, defects. Such a stalling would lead to a relaxation of the stalled front. The new relaxed $\phi(z)$ would then act as the initial condition for the new helicase recruited for repair. The sensitivity to initial condition of a front invading an unstable phase is an important distinction between the metastable (pushed) and the unstable cases. Whether helicases in charge of repair are really sensitive to and recognize these initial conditions need to be probed experimentally.

To summarize, we have proposed a simple coarse-grained model for describing helicase activity on DNA. The DNA is described by a local probability of zipping of the base pairs. The motor action of the helicase induces an instability around the front (Y-fork) in an otherwise coexisting zipped and unzipped phases. Such coexisting phases with an interface can in principle be created by pulling or by a stalled helicase on a dsDNA and therefore can be studied experimentally. We have shown that the local drive created by the helicase leads to a traveling wave solution with a selected velocity that depends on the nature of the drive. Quantitative studies of forces and sensitivity to the initial conditions would provide crucial clues on the nature of dynamics studied in this paper. We hope single molecular experiments in future would be able to probe these in detail.

REFERENCES

[1] ALBERTS B. *et al.*, *Molecular Biology of the Cell*, 4th edition (Garland Publ.) 2002.
[2] VON HIPPEL P. H. and DELAGUOTTE E., *Cell*, **104** (2001) 177; LOHMAN T. M. and BJORNSON K. P., *Annu. Rev. Biochem.*, **65** (1996) 169.
[3] PATEL S. S. and PICHA K. M., *Annu. Rev. Biochem.*, **69** (2000) 651; FASS D., BOGDEN C. E. and BERGER J. M., *Structure*, **7** (1999) 691.
[4] VELANKAR S. S. *et al.*, *Cell*, **97** (1999) 75; SOULTANAS P. *et al.*, *EMBO J.*, **19** (2000) 3799.
[5] SINGLETON M. R. *et al.*, *Cell*, **107** (2001) 79.
[6] LOHMAN T. M., *J. Biol. Chem.*, **268** (1993) 2269.
[7] BHATTACHARJEE S. M. and SENO F., *J. Phys. A*, **36** (2003) L181.
[8] BETTERTON M. D. and JULICHER F., physics/0212045.
[9] CHEN Y. Z. *et al.*, *Phys. Rev. E*, **56** (1997) 919.
[10] BHATTACHARJEE S. M., *J. Phys. A*, **33** (2000) L423 (cond-mat/9912297).
[11] MARENDUZZO D., BHATTACHARJEE S. M., MARITAN A., ORLANDINI E. and SENO F., *Phys. Rev. Lett.*, **88** (2002) 028102.
[12] MARENDUZZO D., TROVATO A. and MARITAN A., *Phys. Rev. E*, **64** (2001) 031901.
[13] SEBASTIAN K. L., *Phys. Rev. E*, **62** (2000) 1128.
[14] KAFRI Y., MUKAMEL D. and PELITI L., *Eur. Phys. J. B*, **27** (2002) 135.
[15] LUBENSKY D. and NELSON D. R., *Phys. Rev. Lett.*, **85** (2000) 1572.
[16] BHATTACHARJEE S. M. and MARENDUZZO D., *J. Phys. A*, **35** (2002) L349.
[17] EBERT U. and VAN SAARLOOS W., *Physica D*, **146** (2000) 1; TRIPATHY G. and VAN SAARLOOS W., *Phys. Rev. Lett.*, **85** (2000) 3556.
[18] BIANCO P. R. *et al.*, *Nature*, **409** (2001) 374; DOHONEY K. M. and GELLES J., *Nature*, **409** (2001) 370.
[19] BENGURIA R. D. and DEPASSIER M. C., *Phys. Rev. Lett.*, **77** (1996) 1171.